

Sodium arsenite exposure inhibits AKT and Stat3 activation, suppresses self-renewal and induces apoptotic death of embryonic stem cells

Vladimir N. Ivanov · Gengyun Wen · Tom K. Hei

Published online: 11 November 2012
© Springer Science+Business Media New York 2012

Abstract Sodium arsenite exposure at concentration $>5 \mu\text{M}$ may induce embryotoxic and teratogenic effects in animal models. Long-term health effects of sodium arsenite from contaminated drinking water may result in different forms of cancer and neurological abnormalities. As cancer development processes seem to be originated in stem cells, we have chosen to examine the effects of sodium arsenite on signaling pathways and the corresponding transcription factors that regulate cell viability and self-renewal in mouse embryonic stem cells (ESC) and mouse neural stem/precursor cells. We demonstrated that the crucial signaling pathway, which was substantially suppressed by sodium arsenite exposure ($4 \mu\text{M}$) in ESC, was the PI3K–AKT pathway linked with numerous downstream targets that control cell survival and apoptosis. Furthermore, the whole core transcription factor circuitry that control self-renewal of mouse ESC (Stat3-P-Tyr705, Oct4, Sox2 and Nanog) was strongly down-regulated by sodium arsenite ($4 \mu\text{M}$) exposure. This was followed by G2/M arrest and induction of the mitochondrial apoptotic pathway that might be suppressed by caspase-9 and caspase-3 inhibitors. In contrast to mouse ESC with very low endogenous IL6, mouse neural stem/precursor cells (C17.2 clone immortalized by *v-myc*) with high endogenous production of IL6 exhibited a strong resistance to cytotoxic effects of sodium arsenite

that could be decreased by inhibitory anti-IL6 antibody or Stat3 inhibition. In summary, our data demonstrated suppression of self-renewal and induction of apoptosis in mouse ESC by sodium arsenite exposure, which was further accelerated due to simultaneous inhibition of the protective PI3K–AKT and Stat3-dependent pathways.

Keywords Embryonic stem cells · AKT · Sodium arsenite · Apoptosis

Abbreviations

EGF	Epidermal growth factor
EGFR	Epidermal growth factor receptor
ESC	Embryonic stem cells
FACS	Fluorescence-activated cell sorter
FGF2	Fibroblast growth factor-2 (basic)
IETD	<i>N</i> -Acetyl-Ile-Glu-Thr-Asp-CHO (aldehyde)
I κ B	Inhibitor of NF- κ B
IGF1	Insulin-like growth factor-1
IGF1R	Insulin-like growth factor-1 receptor
IKK	Inhibitor nuclear factor kappa B kinase
JNK	C-Jun N-terminal kinase
LEHD	<i>N</i> -Acetyl-Leu-Glu-His-Asp-CHO (aldehyde)
MAPK	Mitogen-activated protein kinase
MEK	MAPK/ERK kinase
NF- κ B	Nuclear factor kappa B
NSC	Neural stem cells
PARP-1	Poly(ADP-ribose)polymerase-1
PI	Propidium iodide
PPP	Picropodophyllin
STAT	Signal transducers and activators of transcription
TNF α	Tumor necrosis factor alpha
zVAD	Carbobenzoxy-valyl-alanyl-aspartyl-[<i>O</i> -methyl]-fluoromethylketone

V. N. Ivanov (✉) · G. Wen · T. K. Hei
Department of Radiation Oncology, Center for Radiological Research, College of Physicians and Surgeons, Columbia University, 630 West 168th Street, New York, NY 10032, USA
e-mail: vni3@columbia.edu

Introduction

Arsenic contamination of drinking water is a major environmental problem that affects more than 100 millions of people worldwide. Long-term health effects of inorganic sodium arsenite may result in different forms of cancer and neurological abnormalities [1, 2]. Furthermore, sodium arsenite is a well-characterized teratogen in animal models inducing a general embryotoxicity and causing a substantial disruption in embryonic neurogenesis [3]. However, the precise molecular mechanisms of these effects are still uncertain.

Sodium arsenite at high doses (>10 μM) represents a general cell poison acting in two directions. As a sulfhydryl reagent, arsenite binds to the free thiol (–SH) groups of numerous enzymes inhibiting their activities and also significantly decreasing levels of glutathione (GSH) that further destroys the protective cellular functions [4]. As an inducer of production of reactive oxygen species, sodium arsenite causes oxidative stress, mitochondrial damage and a broad range of pathological conditions. These complementary negative effects of sodium arsenite finally result in the induction of cell death [5–8]. On the other hand, chronic sodium arsenite exposure, which occurred in most cases at low doses (1–5 μM), could notably affect signaling pathways and substantially changing gene regulation in cells, including probably signaling and gene regulation in stem cells. Sodium arsenite is well-documented human carcinogen at these doses in drinking water [2]. As cancer development processes seem to be originated in stem cells [9], we have chosen to examine the effects of sodium arsenite on stem cell viability and self-renewal capacity.

The self-renewal of embryonic stem cells (ESC) and the maintenance of their pluripotency are dependent on multifactorial stimulation of the cell signaling pathways by certain combinations of cytokines and growth factors that control “stemness”-specific gene expression. Even though the combinations of the extrinsic factors are quite different for mouse and human ESC, their downstream targets include similar sets of genes, which encode transcription factors *Oct4*, *Sox2*, *Nanog*, *Klf4* and *cMyc*, the key regulators of pluripotency of ESC [10, 11]. For mouse ESC in culture, external signaling molecules, such as the cytokine leukemia inhibitory factor (LIF) and several growth factors, BMP4, IGF1/2 and Wnt, regulate their self-renewal and pluripotency. Numerous investigations revealed a “minimal” combination of LIF-dependent [12, 13] and BMP-dependent signals [14], which integrate with core transcriptional networks and control the maintenance and proliferation of mouse ESC together with a dynamic inhibition of the differentiation pathways [15–17]. The critical pathways, which regulate the self-renewal of mouse ESC and control gene expression of the core transcription factors, are initiated by LIF:

LIF–(LIFR/gp130)–JAK2–Stat3 and LIF–(LIFR/gp130)–PI3K–AKT, where gp130 is the common signal transduction receptor protein of the IL6 family [13]. The relative pathways could also be initiated by IGF1/IGFR1 or EGF/EGFR. Furthermore, LIF–(LIFR/p130)–Ras–Raf–MEK–MAPK [13] and EGF/EGFR–Ras–Raf–MEK–MAPK signaling pathways are in dynamic crosstalk with Stat3- and AKT-pathways based on mutual interference [15, 16]. In contrast, the BMP–Smad1 pathway appears to suppress differentiation programs of ESC [17].

Experiments with overexpression of gene combinations, encoding specific transcription factors, after retroviral infection of the corresponding cDNA in ESC established several sets of genes: *Oct4*, *Sox2*, *cMyc* and *Klf2* [18, 19]; *Oct4*, *Sox2*, *Lin28* and *Nanog* [20]; *Oct4*, *Sox2*, *Klf4* and *Tbx* [21], which could induce reprogramming fibroblasts to pluripotency. The triumvirate of transcription factors *Oct4*, *Sox2* and *Nanog* plays the fundamental role in gene regulation, often binding multiple closely localized sites in the regulatory regions of the genome, creating enhanceosomes and coordinating expression of numerous genes in ESC. *Smad1*, *Stat3* and the coactivator p300 appear to be additional components of enhanceosomes [17, 22].

The main hypothesis, which had been addressed in the present study, was that sodium arsenite might directly target numerous signaling pathways in ESC, suppressing self-renewal and promoting apoptosis. To prove our hypothesis, we elucidated the effects of sodium arsenite exposure on signaling pathways in mouse ESC with a special attention to regulation of expression levels of key transcription factors *Oct4*, *Sox2* and *Nanog*.

During embryogenesis, sodium arsenite, which is known as transplacental carcinogen [23], might affect survival and proliferation of different types of stem/precursor cells, including embryonic neural stem/precursor cells, which can differentiate into the cells in the nervous system. We have further suggested in the present study that sodium arsenite exposure might target the embryonic neurogenesis in mice via interference and interaction with cell signaling pathways in mouse neural stem/precursor cells. We also elucidate a possible mechanism of the resistance to apoptotic death induced by sodium arsenite in neural stem/precursor cells based on the IL6–Stat3 pathway.

Results

Sodium arsenite treatment modulates signaling pathways that control self-renewal and survival of mouse ESC

In mouse ESC exposed to graded doses of sodium arsenite (1–6 μM , 24–48 h), there was a dramatic dose-dependent

reduction in cell survival as shown in Fig. 1. Phase contrast microscopy of live cell cultures demonstrated a massive flotation of ESC (24–48 h after treatment) that was accompanied by cell death (Fig. 1a). Annexin-V-FITC and PI staining of control and sodium arsenite treated ES cells revealed an increase in percentage of Annexin-V-FITC-positive apoptotic cells (most of which were also PI-positive) 12 h after treatment with the coincident increase in the subpopulation of the secondary necrotic (Annexin-V-FITC-negative, PI-positive) cells (Fig. 1b). Simultaneously, we observed significant changes in expression levels of hallmark proteins that control cell survival and apoptosis, such as a upregulation of the protective enzyme, heme oxygenase-1 (HO-1), that linked with massive heme inactivation after cytochrome-*c* release from mitochondria,

transcription factor FOXO3A (as a sensor of oxidative stress), p21-WAF (as an indicator of the cell cycle arrest) and, finally, caspase-3-mediated PARP-1 cleavage (as an indication of irreversible apoptotic commitment) (Fig. 1c).

FACS assays of PI-stained nuclei revealed strong dose-dependent changes in cell cycle regulation for stem cells that resulted in G2/M arrest 24 h after arsenic treatment followed by pronounced apoptosis 48 h after treatment (Fig. 1d–f). As expected, total levels of cell death were higher, than apoptotic levels after sodium arsenite exposure of mouse ESC, due to induction of necrosis (Fig. 1d). A relative resistance of normal cells, including embryonic fibroblasts, to the cytotoxic effects of sodium arsenite at low doses (<5 μM) is well-known phenomenon [24],

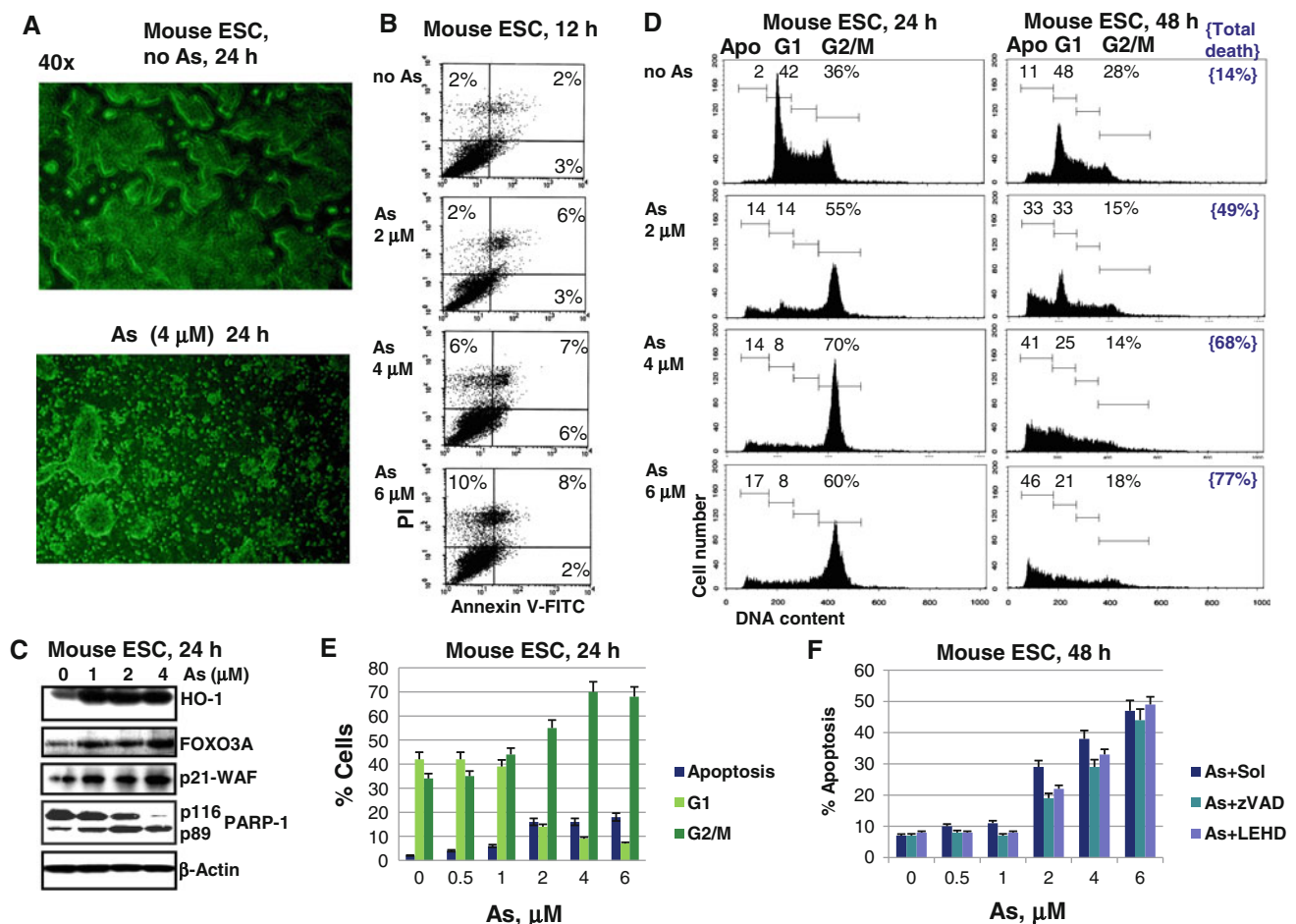


Fig. 1 Sodium arsenite treatment of mouse ESC induced G2/M arrest followed by apoptotic cell death. **a** Phase contrast microscopy ($\times 40$ magnification) of mouse ESC (cultured as adherent cells) in the absence and in the presence of 4 μM sodium arsenite, 24 h of exposure. **b** Annexin-V-FITC and PI staining of control and arsenite-treated ESCs was followed by FACS analysis. **c** Western blot analysis of expression of indicated proteins in mouse ESC 24 h after treatment by increasing doses of sodium arsenite. β -Actin was used as a loading control. **d–f** Cell cycle-apoptosis analysis of mouse ESC 24–48 h

after treatment with sodium arsenite (2–6 μM). Cells were stained by propidium iodide and analyzed by the flow cytometry. A typical experiment is presented in (b); pooled results of four independent experiments are shown in (c). *Error bars* represent means \pm SD ($p < 0.05$, Student's *t* test). **e** Effects of a universal caspase inhibitor zVAD-fmk (40 μM), a caspase-9 inhibitor Ac-LEHD-CHO (40 μM) and vehicle solution (sol) that contained 0.1 % DMSO on arsenite-induced apoptosis in mouse ESC. *Error bars* represent means \pm SD ($p < 0.05$, Student's *t* test)

which allows us to use arsenic for treatment of sensitive types of cancer without strong cytotoxicity for normal cells [25, 26]. On the other hand, a higher sensitivity of ESC to arsenic exposure described in the present study increases our understanding of risks linked with such treatment.

Sodium arsenite (especially at doses $>5 \mu\text{M}$) could directly target mitochondria causing mitochondrial damage, cytochrome-*c* release to the cytoplasm and initiating the caspase-9-mediated mitochondrial death pathway [27, 28]. We used a pan-caspase inhibitor zVAD-fmk (50 μM) and specific caspase-9 inhibitor Ac-LEHD-CHO (50 μM), to obtain further evidences of activation of the mitochondrial apoptotic pathway in mouse ESC after arsenite treatment. Both inhibitors, zVAD-fmk and Ac-LEHD-CHO, notably suppressed apoptotic death induced by 1–4 μM sodium arsenite, while for higher arsenic concentration their inhibitory effects were not pronounced (Fig. 1f) indicating on increased levels of non-apoptotic cell death. Caspase-8 inhibitor Ac-IETD-CHO did not exhibit substantial effects on apoptosis in ESC (data not shown), further highlighting a role for induction of the mitochondrial apoptotic pathway after sodium arsenite treatment [28, 29].

In contrast to many cancer cell lines, transfer of ES cells to the restricted media (with 1 % FBS but without LIF) rapidly induced cell floating and high levels of cell death by apoptosis (Fig. 2b, c). In the presence of sodium arsenite (2 μM), already high levels of spontaneous apoptotic death of ES cells grown in 1 % FBS were only modestly elevated (Fig. 2b, c). On the other hand, a combination of less restricted media (with 7.5 % FBS, without LIF) and sodium arsenite demonstrated additive increase in apoptotic levels of ECS (Fig. 2b). Combined treatment notably changed the protein levels of FGFR1 and EGFR, but not IGFR1, which could further down-regulate activating signaling in ESC at the late time points (Fig. 2a). In summary, these observations indicated that sodium arsenite exposure and growth factor withdrawal had the same final destination, induction of apoptosis, which could be mediated by the similar signaling pathways.

Sodium arsenite exposure of ESC in the complete media induced a transient activation of JNK and c-Jun that was characteristic for the relatively early time point of 3–6 h after treatment and was followed by gradual down-regulation of JNK activity (Fig. 3a). On the other hand, the PI3K–AKT connection, a cross-road of signaling pathways induced by activated growth factor receptor protein kinases (such as IGFR and EGFR) or by LIF receptor complex, plays a central role for a general cell survival and anti-apoptotic protection [30]. Our experiments demonstrated negative properties of sodium arsenite treatment on the late AKT activation (16–24 h of exposure) via inhibition of its Ser473 phosphorylation (Fig. 3a, b). As expected,

Fig. 2 Effects of low serum media and sodium arsenite on cell cycle and apoptosis of mouse ESC. **a** Western blot analysis of expression levels of growth factor receptors in mouse ESC 24 h after treatment with 2 μM sodium arsenite in the media with 15 % or with 1 % FBS. **b** Cell cycle-apoptosis analysis of mouse ESC 24 h after treatment with sodium arsenite (1–2 μM) in three types of media: with 15 % FBS, 7.5 % FBS and 1 % FBS. Cells were stained by propidium iodide and analyzed by the flow cytometry. **c** Phase contrast microscopy ($\times 80$ magnification) of mouse ESC (cultured as adherent cells) in media with 15 % FBS or 1 % FBS in the absence or in the presence of 2 μM sodium arsenite, 24 h of exposure

suppression of AKT after 16 h of arsenic exposure was also accompanied by down-regulation of protein expression levels of β -catenin (Fig. 3a) that could be protected from degradation via AKT-mediated inactivation of GSK3 β [31]. We and others previously reported a negative regulation of Jak2/Stat3 in normal and cancer cells by sodium arsenite treatment [26, 32]. We further demonstrated the negative effects of sodium arsenite treatment on Stat3 activation via Tyr705 phosphorylation in mouse ESC (Fig. 3a). Since LIF–Jak2–Stat3 activation is crucial for ESC proliferation and survival [12, 13], negative effect of sodium arsenite exposure on Stat3 activation are significant for acceleration of arsenite-induced apoptosis in ESC. Furthermore, sodium arsenite exposure persistently upregulated already high basal levels of MEK-dependent ERK1/2 activity. In contrast to JNK activation, high levels of active phospho-ERK1/2 were detected in ESC even 16 h after treatment (Fig. 3a).

Protein levels of transcription factors Oct4, Sox2 and Nanog, which together with Stat3 and c-Myc were assembled in the core transcription factor circuitry of ESC [12], started to decrease in dose-dependent manner 6 h after sodium arsenite treatment; this decrease was well pronounced 16 h after treatment (Fig. 3a). It reflected a new balance between expression of genes, encoding *Oct4*, *Sox2* and *Nanog*, and the corresponding protein degradation that was established in conditions of sodium arsenite exposure. Quite surprisingly, total p53 levels were relatively stable after sodium arsenite exposure (Fig. 3a) without a notable effect on its Ser15/Ser20 phosphorylation (data not shown). We also did not observe any substantial effects of low doses (2–4 μM) of sodium arsenite on IKK activation via suppression of its phosphorylation, as well as on the subsequent I κ B α phosphorylation mediated by IKK β in ESC. Even though BMS345541 (10 μM), a specific inhibitor of the IKK–NF- κ B pathway, demonstrated strong negative effects in ESC and finally down-regulated levels of the nuclear NF- κ B p65-(phospho-Ser536) subunit (Fig. 3c).

An additional usage of specific inhibitors of tyrosine kinase activity of growth factor-receptors, which control proliferation and survival of ESC, demonstrated strong negative effects of PPP, an inhibitor of IGF1R kinase

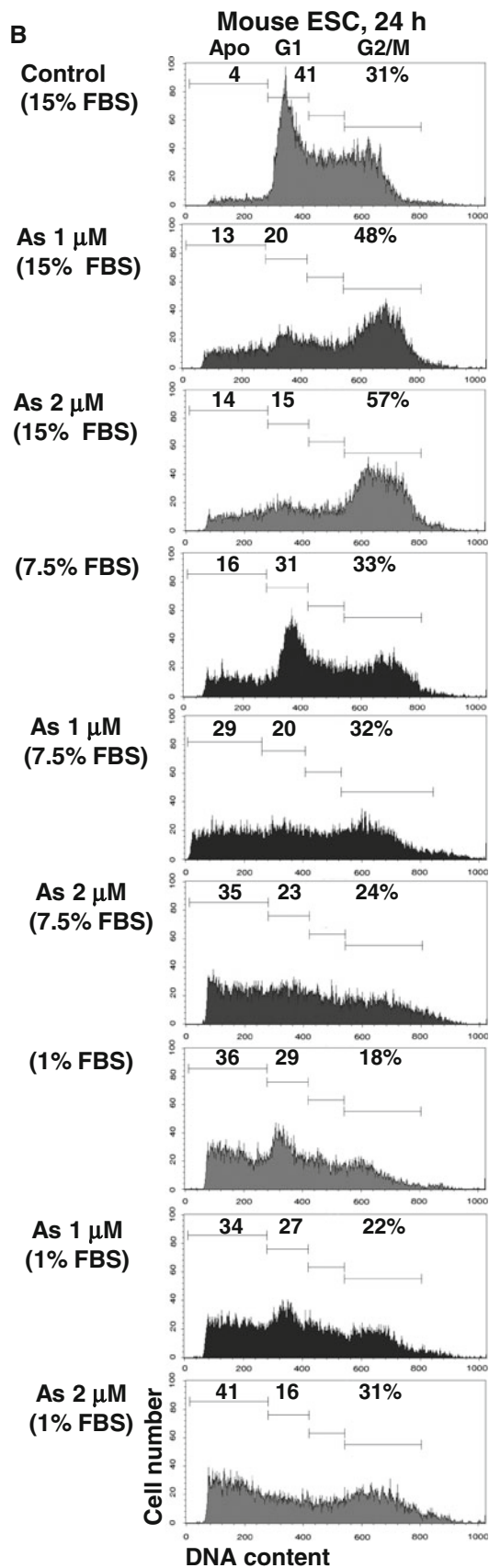
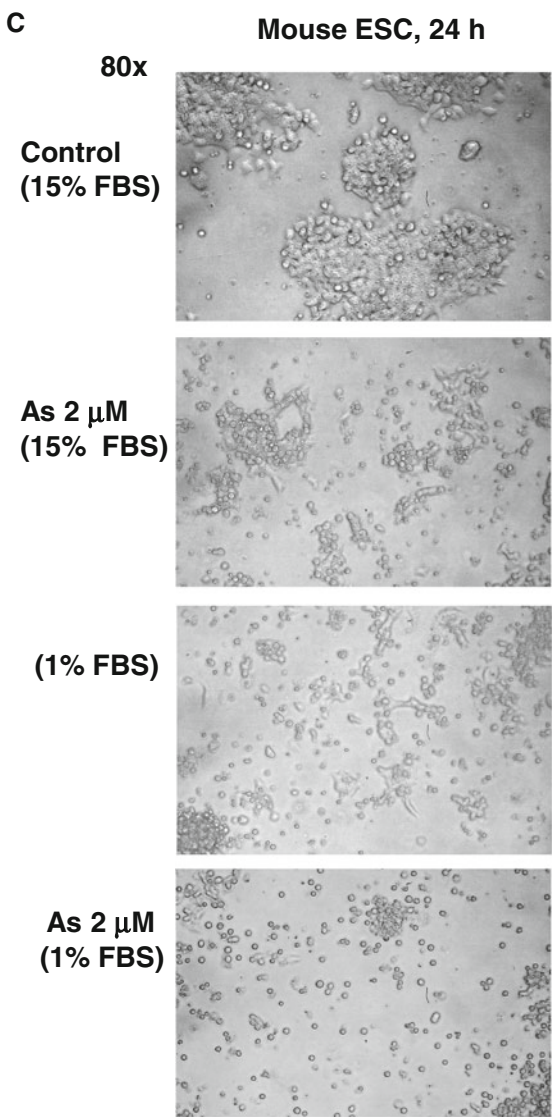
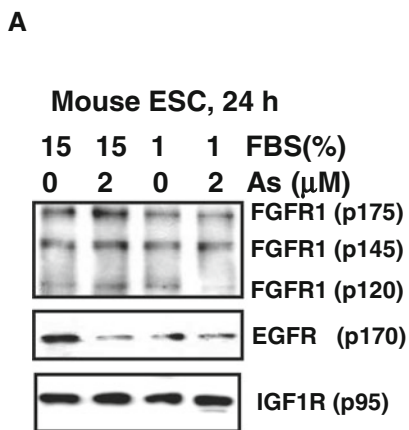
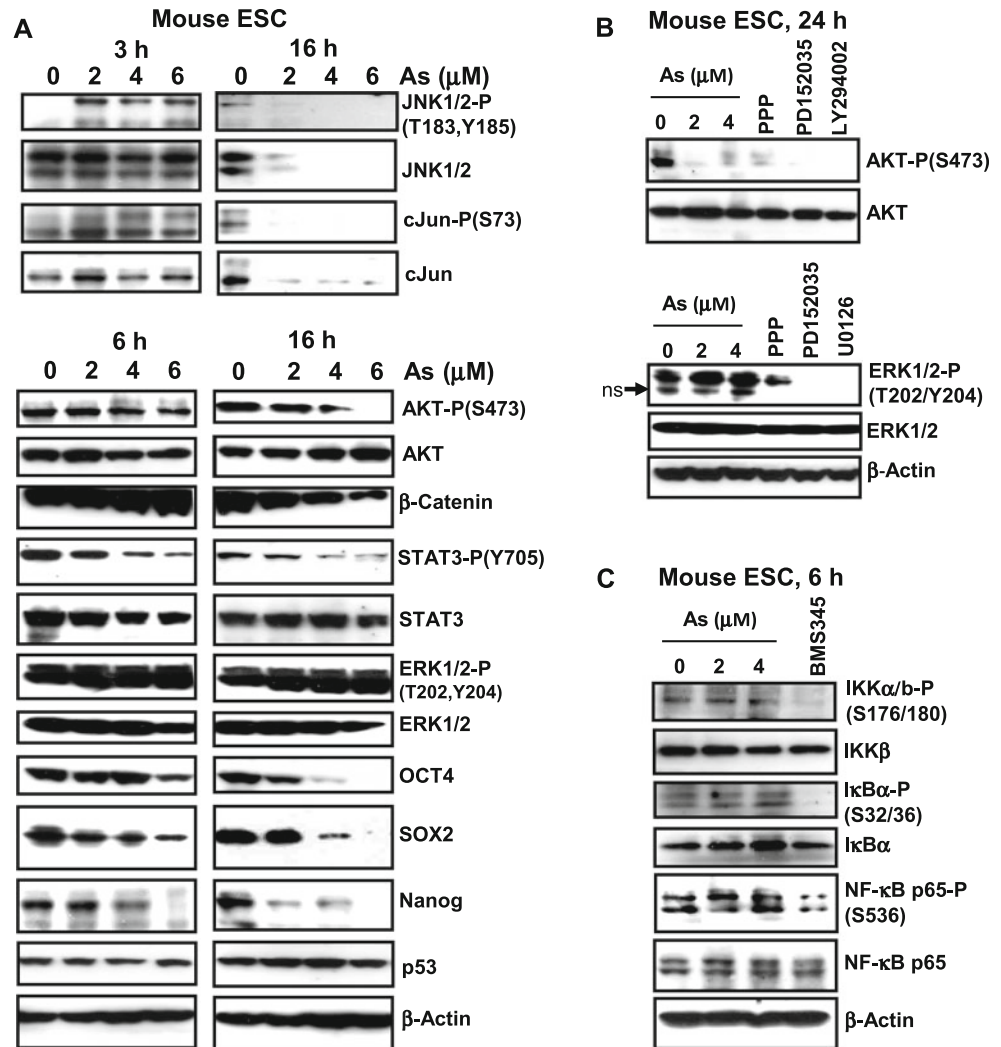


Fig. 3 Effects of sodium arsenite treatment on signaling pathways and corresponding transcription factors in mouse ESC. **a–c** Western blot analysis of indicated proteins was performed 3, 6, 16 and 24 h after treatment with increased doses of sodium arsenite. Panels **(b)** and **(c)** demonstrate effects of small molecule inhibitors of cell signaling pathways: PPP (0.5 μ M), an inhibitor of IGF1R protein kinase activity; PD153035 (20 μ M), an inhibitor of EGFR protein kinase activity; LY294002 (40 μ M), an inhibitor of PI3K–AKT; U0126 (10 μ M), an inhibitor of MEK–ERK; BMS345541 (10 μ M), an inhibitor of IKK–NF- κ B. All inhibitors were dissolved in 0.1 % DMSO; control cultures were treated with 0.1 % DMSO



activity, on activation of PI3K–AKT. PD152035, an inhibitor of EGFR kinase activity, as well as LY294002, an inhibitor of PI3K, exhibited similar effects that finally coincided with effects of sodium arsenite 24 h after treatment (Fig. 3b). As expected, MEK–ERK activation was also dependent from activation of both IGF1R- and especially EGFR-dependent signaling pathways, as was shown by negative effects of specific upstream inhibitors, PPP and PD152035, on these signaling pathways. Small molecule inhibitor of MEK, U0126 (10 μ M), blocked MEK–ERK activation that was opposite to arsenite action (Fig. 3b, the bottom panel).

To further evaluate effects of sodium arsenite on cell signaling, we compared its action with effects of specific molecule inhibitors on regulation of the cell cycle and apoptosis in ESC. The rapid response with pronounced induction of apoptosis in ESC was observed for LY294002 (40 μ M), a PI3K–AKT inhibitor, and BMS345541 (10 μ M), an IKK–NF- κ B inhibitor (Fig. 4a, b). Furthermore, PPP and PD153035, inhibitors of IGF-1R and EGFR

kinase activity, respectively, and upstream suppressors of AKT activation, induced strong changes in the cell cycle distribution and high levels of apoptosis (Fig. 4a, b). Inhibition of Stat3 with Stat3-inhibitor-6 (50 μ M) also resulted in notably increased levels of apoptosis (Fig. 4b). In contrast, suppression of MEK–ERK by U0126 increased G1 arrest and induced a modest apoptosis. SP600125, a JNK inhibitor, and SB203580, a MAPK p38 inhibitor, did not increase basal levels of apoptosis (Fig. 4b). Caspase-3-dependent cleavage of PARP-1 provided a further proof of apoptotic commitment in ESC induced by LY294002 and BMS345541 (Fig. 4c). Taken together, these data indicated that suppression of PI3K–AKT and Stat3-mediated signaling by sodium arsenite treatment of ESC could be critical for deregulation of the cell cycle and the subsequent apoptosis.

Inhibition of IKK–NF- κ B also substantially decreased survival of ESC (Fig. 4a, b). A general protective function of NF- κ B in embryogenesis, especially in neurogenesis, is well known [33]. However, sodium arsenite treatment at

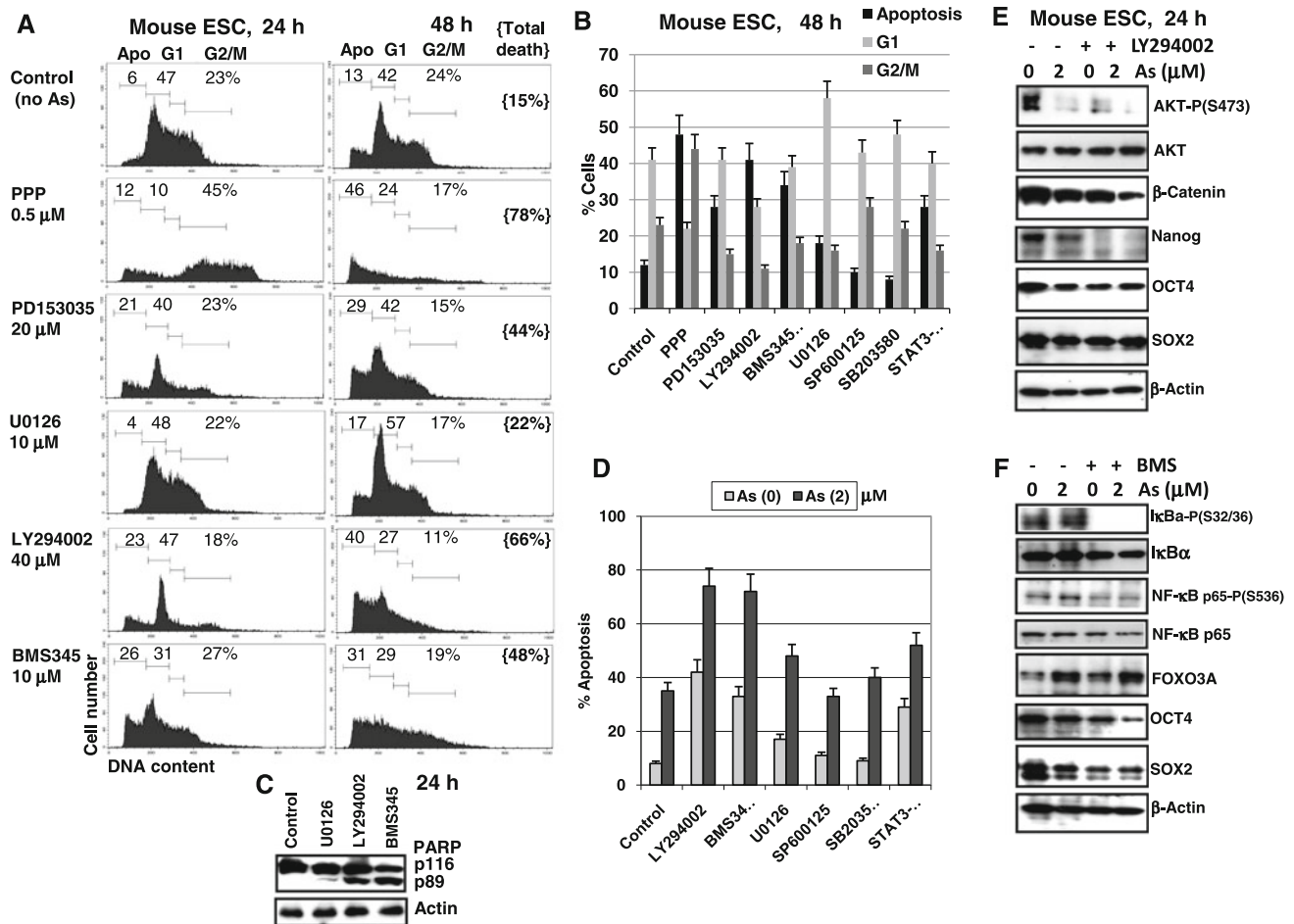


Fig. 4 Effects of small molecule inhibitors of signaling pathways on cell cycle and apoptosis of mouse ESC. Inhibitors of main signaling pathways used are: PPP (0.5 μ M), an inhibitor of IGF-1R protein kinase activity; PD153035 (20 μ M), an inhibitor of EGFR protein kinase activity; LY294002 (40 μ M), an inhibitor of PI3K–AKT; BMS345541 (10 μ M), an inhibitor of IKK–NF- κ B; U0126 (10 μ M), an inhibitor of MEK-ERK; SP600125 (20 μ M), an inhibitor of JNK; SB203580 (40 μ M), an inhibitor of MAPK p38; and STAT3 inhibitor-6 (20 μ M). All inhibitors were dissolved in 0.1 % DMSO; control cultures were treated with 0.1 % DMSO. **a**, **b** Cell cycle-apoptosis analysis of mouse ESC 24–48 h after treatment with a specific inhibitor of signaling pathway. Treated cells were stained by propidium iodide and analyzed by flow cytometry. A typical experiment (one from four) is presented in (**a**); pooled results of

four independent experiments are presented in (**b**). Error bars represent means \pm SD ($p < 0.05$, Student's *t* test). Total death levels were determined by cell counting using trypan blue staining and light microscopy. **c** Western blot analysis of caspase-3-dependent PARP-1 cleavage was performed 24 h after exposure to indicated inhibitors. β -Actin was used as a loading control. **d** Cell cycle-apoptosis analysis of mouse ESC 48 h after treatment with specific molecule inhibitors of cell signaling in the presence or in the absence of sodium arsenite (2 μ M); control cultures were treated with 0.1 % DMSO alone or in combination with sodium arsenite. Error bars represent means \pm SD ($p < 0.05$, Student's *t* test). **e**, **f** Western blot analysis of protein expression levels 24 h after treatment of mouse ESC with sodium arsenite (2 μ M), LY294002 (40 μ M), BMS345541 (10 μ M) alone or in combination

low doses did not notably affect the NF- κ B pathway and NF- κ B-dependent transcription in ESC (see Fig. 3c). In contrast to numerous cancer lines, the NF- κ B pathway in ESC probably does not critically involve regulation of the resistance to sodium arsenite. Interestingly, the summary effects of sodium arsenite treatment on regulation of the ESC cell cycle-apoptosis were quite similar to an upstream inhibition of IGR1/IGF1R-mediated signaling by PPP. Related results with final induction of apoptosis were also obtained after EGF/EGFR inhibition (Fig. 4a, b). Quite surprisingly, that in spite of common downstream targets,

suppression of either IGFR1 or EGFR resulted in pronounced apoptosis in ESC, indicating incomplete interchangeability of the signaling pathways initiated by these receptor protein kinases.

Next, we evaluated effects of a relatively low dose of sodium arsenite (2 μ M) in combination with inhibitors of signaling pathways on self-renewal and apoptosis in mouse ESC, as well as on protein expression levels of key transcription factors, Oct4, Sox2 and Nanog. Treatment of ESC with sodium arsenite (2 μ M) in combination either with LY294002, or with BMS345541 additively increased

apoptotic levels, achieving or surpassing levels induced by 6 μM sodium arsenite alone (Fig. 4d). Some enhancing effects on arsenite-induced apoptosis were observed with U0126 and Stat3-inhibitor-6, while SP600125 and SB203580 did not exhibit notable effects (Fig. 4d).

LY294002 alone or in combination with sodium arsenite (2 μM) strongly decreased protein levels of Nanog (Fig. 4e). Positive regulation of Nanog expression by PI3K–AKT signaling via inhibition of GSK3 was previously described [34]. In contrast, LY294002 and sodium arsenite (2 μM) only modestly decreased Oct4 and Sox2 levels, acting alone or in combination. On the other hand, additive negative effects of LY294002 and sodium arsenite were observed for β -catenin protein levels, highlighting again a role of PI3K–AKT–GSK3 β in stabilization of β -catenin protein levels and a role of sodium arsenite as an inhibitor of this pathway (Fig. 4e).

BMS345541 alone or especially in combination with sodium arsenite (2 μM) strongly decreased Oct4 protein expression, revealing a possible role of IKK–NF- κB (in concert with other transcription factors) for control of Oct4 expression. Both agents also decreased Sox2 levels, but without additive effects in combination (Fig. 4f). On the other hand, upregulation of transcription factor FOXO3A protein levels induced by sodium arsenite was not affected by simultaneous BMS345541 treatment (Fig. 4f). Results obtained exhibited relatively mild effects of lower doses of sodium arsenite (1–2 μM) on key transcription factors in ESC; however, an increase in concentration of sodium arsenite (up to 4–6 μM) resulted in a significant down-regulation of the levels of key transcription factors, Oct4, Sox2 and Nanog (see Fig. 3). So, protein levels of β -catenin, Nanog and Oct4 were under control of the PI3K–AKT pathway; furthermore, Oct4 and Sox2 levels were also dependent from IKK–NF- κB in mouse ESC. Combinations of sodium arsenite (2 μM) with either LY294002 or BMS345541 demonstrated additive suppression of β -catenin and Oct4 levels, respectively.

We also evaluated a role for mTOR in response of ESC to arsenic exposure. Activation of mTOR, a key regulator of protein synthesis in the cell, is a well-known downstream effect of the PI3K–AKT pathway [35]. Our data further demonstrated negative effects of sodium arsenite treatment (24–48 h) on the late AKT activation through inhibition of Ser473 phosphorylation and the subsequent down-regulation of its downstream target, mTOR activation, in ESC 24 h after treatment (Fig. 5a, b). We also expected that sodium arsenite-mediated suppression of mTOR activity was critically involved in the regulation of arsenite-induced apoptosis. Surprisingly, rapamycin (1–5 nM), a specific inhibitor mTOR activity, induced G1 arrest of the ESC proliferation, rather than apoptosis (Fig. 5b). It probably indicated a significance of other

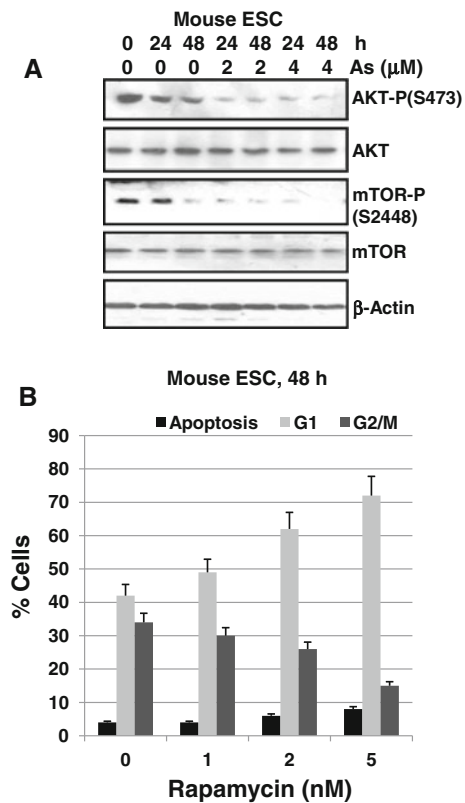


Fig. 5 Sodium arsenite exposure suppresses mTOR activation in mouse ESC. **a** Western blot analysis of indicated proteins was performed 24 and 48 h after treatment with increased doses of sodium arsenite (0, 2 and 4 μM). **b** Cell cycle-apoptosis analysis of mouse ESC 48 h after treatment with rapamycin (1–5 nM), a mTOR inhibitor. Cells were stained by propidium iodide and analyzed by the flow cytometry. Pooled results of four independent experiments are shown. Error bars represent means \pm SD ($p < 0.05$, Student's t test)

downstream targets of AKT in regulation of anti-apoptotic response.

In summary, our data demonstrated profound, but differential effects of sodium arsenite exposure on cell signaling pathways regulating the cell cycle, general cell survival and apoptosis in mouse ESC, balancing between cell cycle arrest, apoptosis and differentiation.

Effects of sodium arsenite exposure on immortalized mouse neural stem/progenitor cells (clone C17.2)

We used in our study surrogate mouse neural stem/progenitor cells (C17.2), which were isolated from neonatal mouse cerebellum. Propagation and stem-like behavior of this cell line was augmented via *v-myc* transduced by MMLV retrovirus vector [36]. Interestingly, the DNA profile of these cells, which were stained with PI, indicated a high level of aneuploidy (Fig. 6a). It was correlated with results of the former study that detected aneuploidy in

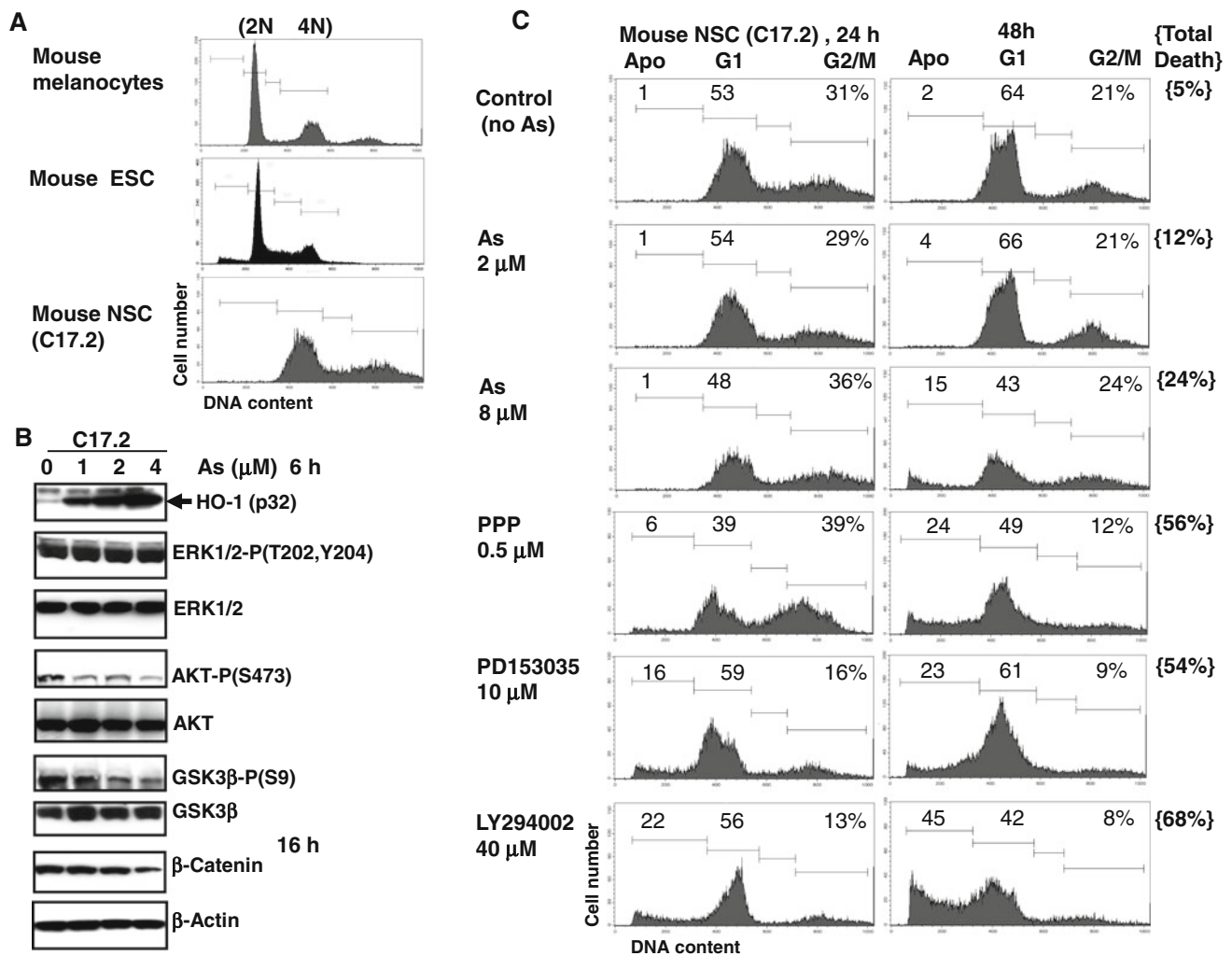


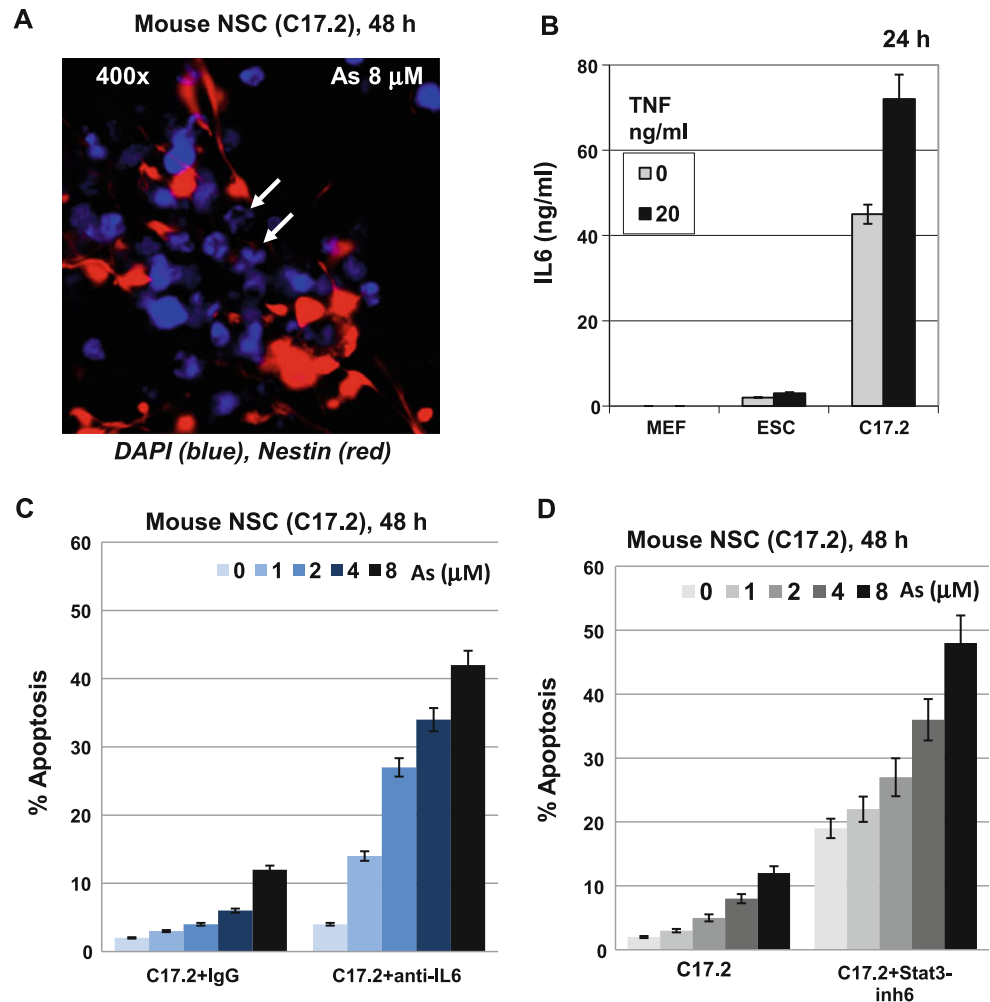
Fig. 6 Effects of sodium arsenite exposure on mouse neural stem/precursor cells (C17.2). **a** Comparison of DNA content of mouse cell lines using PI staining and FACS analysis. **b** Western blot analysis of indicated proteins after arsenic treatment of C17.2 cells. **c** Cell cycle-

apoptosis analysis of C17.2 cells 24–48 h after indicated treatment. Cells were stained by propidium iodide and analyzed by the flow cytometry. Total cell death levels were determined using Trypan blue staining

C17.2 cells using chromosome staining [37]. Unexpectedly, our data demonstrated a high resistance of C17.2 cells to sodium arsenite-induced apoptosis in culture conditions: modest apoptotic levels were detected only 48 h after arsenite treatment at dose 8 μM (Figs. 6c, 7a). A recent study also proven anti-apoptotic resistance of C17.2 cells, demonstrating pronounced apoptosis at extremely high doses of sodium arsenite, such as 40 μM [38]. In contrast, LY294002, a PI3K–AKT inhibitor, and two upstream inhibitors of PI3K–AKT signaling, PPP and PD153035, were able to induce pronounced apoptosis in C17.2 cells 48 h after treatment (Fig. 6c). As expected, total cell death levels were higher than apoptotic levels in treated C17.2 cells (Fig. 6c). Western blot assay revealed very high basal levels of active ERK1/2, which were further upregulated by arsenite, but modest levels of active AKT-phospho-Ser473 that were downregulated by sodium arsenite exposure. It

was accompanied by a partial suppression of GSK3 β phosphorylation and relatively modest down-regulation of β -Catenin protein levels (Fig. 5b). Inducible expression of HO-1, a hallmark protective enzyme, served as an internal control of initiation of arsenite-dependent intracellular activities (Fig. 6b). What was a reason for substantial resistance of C17.2 cells to sodium arsenite treatment? Previously performed profiling of gene expression in C17.2 cells demonstrated massive changes in gene expression, including increased production of IL6 in this cell line, compared to the primary mouse neural stem cells [37]. Mouse ESC, which are critically dependent on the exogenous LIF, an IL6-related cytokine, also produce very low levels of the endogenous IL6 [39]. We further confirmed these data detecting the high basal and TNF α -induced levels of IL6 secretions in the culture media of C17.2 cells, compared to MEF or ESC (Fig. 6b). Addition of anti-IL6

Fig. 7 Upregulation of apoptosis in mouse neural stem cells through inhibition of IL6. **a** Nestin (red) immunostaining and DAPI (blue) staining of mouse NSC (C17.2) 48 h after sodium arsenite (8 μ M) exposure. Apoptotic nuclei are shown by the white arrows. **b** Levels of IL6 (ng/ml) in the culture media of non-treated or TNF α -treated MEF, ESC and C17.2 (500,000 cells/well) were determined by ELISA 24 h after treatment. **c** Dose-dependent levels of apoptosis (determined by PI staining with the subsequent FACS assay) in mouse C17.2 cells 48 h after sodium arsenite exposure. Anti-IL6 inhibitory antibody or control IgG (5 μ g/ml) were added to C17.2 cells before sodium arsenite treatment. **d** Effect of Stat3-inhibitor-6 (20 μ M) on sodium-arsenite induced apoptosis in C17.2 cells 48 h after treatment. Error bars in the (b)–(d) represent means \pm SD ($p < 0.05$, Student's *t* test) (Color figure online)



inhibitory mAb (5 μ g/ml) into the culture media substantially increased levels of sodium arsenite-induced apoptosis in C17.2 cells (Fig. 7c), highlighting a protective effect of the endogenous production of IL6. Since IL6 is a powerful inducer of Stat3 activation, we further treated C17.2 cells with Stat3-inhibitor-6 (20 μ M) alone or in combination with sodium arsenite, significantly increasing the basal and arsenite-induced levels of apoptosis (Fig. 7d). It also demonstrates a protective role of IL6-induced Stat3 activation against arsenite-induced apoptosis. Taken together, our results and published data allow us to consider C17.2 cells as model line with a strong resistance to sodium arsenite exposure in vitro, due to upregulation of IL6-Stat3-dependent signaling.

Discussion

A positive role of the PI3K–AKT pathway in regulation of embryonic stem cell and neural stem cell self-renewal has been well established [34, 40–42]. Two specific targets of

this pathway are the “stemness” factors Nanog and Oct4 in mouse ESC [34]. Furthermore, the PI3K–AKT pathway is involved in regulation of numerous cell functions, including activation of mTOR that regulates a general protein synthesis in the cell [35]. A significance of PI3K–AKT/ β -catenin and Wnt/ β -catenin signaling in the maintenance of self-renewal of ESC and NSC cells was also elucidated in detail [43, 44]. Suppression of GSK3 β activity by AKT that resulted in stabilization of protein levels of β -catenin and cyclin D1 was one of the critical events in regulation of proliferation and survival of neural stem cells [45]. There is no surprise that cancer cells do use the same strategy for increasing proliferation and survival based on activation of the PI3K–AKT pathway [46].

The results of the present study also indicated that one of the main and common targets for negative regulation by sodium arsenite was the PI3K–AKT pathway in both mouse ESC and NSC. Consequently, the current data and previous studies demonstrated that efficient protection against sodium arsenite action in ESC, NSC and in numerous cancer cell lines might be achieved by

over-activation of the PI3K–AKT pathway [41, 47]. This pathway could be permanently induced in cells by variety of growth factors and cytokines, such as LIF, FGF2, EGF and IGF1/2, which could be present in the complete media in vitro, by these growth factors produced by helper cells of microenvironment or by endogenously produced growth factors via cell paracrine and autocrine mechanisms in vivo. In contrast, a general inhibition of the PI3K–AKT pathway by LY294002 or by sodium arsenite (but not mTOR inhibition) induced pronounced apoptosis that was additively increased by combined treatment using both agents. Arsenite-induced mitochondrial damage, the subsequent cytochrome-*c* release and caspase-9/caspase-3 mediated apoptosis could substantially decrease a survival of mouse ESC after sodium arsenite exposure.

Effects of sodium arsenite on its downstream targets in ESC were further investigated in the present study. Besides negative regulation of targets of the PI3K–AKT pathway, such as Oct4 and Nanog, sodium arsenite exposure further down-regulated the Jak2–Stat3 pathway and its downstream targets, including Stat3/Oct4-dependent expression of Sox2 in ESC. It finally suppressed the whole core transcription factor circuitry that control self-renewal of mouse ESC, including Stat3, Oct4, Sox2 and Nanog [12, 22].

Negative regulation of IKK–NF- κ B activities by sodium arsenite (5–10 μ M) is a well-established phenomenon for many normal and cancer cell lines [48, 49]. However, for ESC investigated in the present study, sodium arsenite (2–4 μ M) actually did not affect IKK–NF- κ B activation, due to probably increased compensatory production of endogenous cytokines, including TNF α [50] that by itself was a powerful inducer of the NF- κ B activation pathway. This problem, however, needs a more precise analysis, since numerous protein–protein interactions of key transcription factors, such as Stat3–NF- κ B p65 [51] or Stat3–Nanog [52] could substantially complicate general regulation of NF- κ B-dependent and Stat3-dependent gene expression in stem cells.

In contrast to ESC, immortalized mouse neural stem/precursor cells C17.2 demonstrated a high resistance to sodium arsenite exposure (see Fig. 6c). However, this situation is based on massive changes in gene regulation for immortalized mouse NSC (C17.2), compared to the primary neural stem cells, including strongly increased endogenous production of IL6 [37]. This reminds a correlation between N-Myc amplification/overexpression and a strong IL6 production by human neuroblastomas [24, 53]. Indeed, using anti-IL6 antibody, we increased a sensitivity of C17.2 cells to sodium arsenite-mediated apoptosis. Suppression of the main downstream signaling target of IL6, Stat3, by specific small molecule inhibitor also substantially upregulated arsenite-induced apoptosis in C17.2 cells (Fig. 7c, d).

Sodium arsenite was previously described as a two-sided sword, which is a well-known human carcinogen and an effective therapeutic agent for treatment of some types of cancer, especially for treatment of acute promyelocytic leukemia [25]. Better understanding of mechanisms of cytotoxic action of sodium arsenite, for example, in the nervous system and narrowing the window of its specific effects for cancer, such as neuroblastoma [54], is a priority for the development the anti-cancer therapy.

Materials and methods

Materials

Sodium arsenite, fibronectin, laminin and polyornithine were obtained from Sigma-Aldrich (St. Louis, MO, USA). PI3K inhibitor LY294002, IKK inhibitor BMS-345541, STAT3 inhibitor-6 S3I-201 (also known as NSC 74859), IGF-1R kinase inhibitor picropodophyllin (PPP), PI3K inhibitor LY294002, MEK inhibitor U0126, MAPK p38 inhibitor SB203580 and caspase inhibitors zVAD-fmk, LEHD and IETD were purchased from Calbiochem (La Jolla, CA, USA). Annexin-V-FITC was obtained from BD Bioscience (San Jose, CA, USA).

Maintenance of mouse ESC

We used in the present study ESC line W4 from 129/SvEvTac mice. Mouse ESC were grown in DMEM with 15 % FBS, 1 % glutamine, 1 % nonessential amino acids, 0.1 mM β -mercaptoethanol, and 10^5 U/ml LIF (ESGRO) on fibronectin coated dishes.

Maintenance of mouse neural stem cells (C17.2), mouse embryonic fibroblasts and mouse melanocytes

Mouse surrogate neural stem cells (C17.2 clone) and mouse embryonic fibroblasts (MEF) were grown in DMEM with 15 % FBS, 1 % glutamine, and 1 % penicillin/streptomycin. The neural stem cells (C17.2 clone) were kindly provided by Dr. E.Y. Snyder (Sanford-Burnham Research Institute, San Diego, CA). Mouse melanocytes were grown in TICVA medium.

Immunocytochemistry analysis

Cells were fixed with 4 % paraformaldehyde in PBS for 60 min. Immunocytochemical staining was performed using standard protocols. Cells were stained for the undifferentiated NSC marker, nestin (using mAb from Millipore, Temecula, CA, USA) and for localization of the nuclei using DAPI.

Apoptosis studies

For induction of apoptosis, cells were exposed to sodium arsenite (1–10 μM) alone or in the presence of small molecule inhibitors of cell signaling pathways. Apoptosis was then assessed by PI staining and quantifying the percentage of hypodiploid nuclei (pre-G1) or by quantifying the percentage of AnnexinV-FITC-positive cells, both PI-negative and PI-positive. Flow cytometric analysis was performed on a FACS Calibur flow cytometer (Becton–Dickinson) using the CellQuest program. Determination of total cell death levels was performed by Trypan blue staining.

Western blot analysis

Total cell lysates (50 μg protein) were resolved on SDS-PAGE, and processed according to standard protocols. The monoclonal antibodies used for western blotting included: anti- β -actin (Sigma, St. Louis, MO, USA); anti-caspase-8, anti-caspase-9, anti-caspase-3 (Cell Signaling, Danvers, MA, USA); The polyclonal antibodies used included anti-phospho-p44/p42 MAP kinase (T202/Y204) and anti-p44/p42 MAP kinase; anti-phospho-JNK and anti-JNK1-3; anti-phospho-cJun (S73) and anti-cJun; anti-phospho-AKT (S473) and anti-AKT; anti-phospho-p65 (S536) NF- κ B and anti-p65 NF- κ B, anti-phospho-STAT3 (Y705) and anti-STAT3; anti-phospho-FOXO3A (S253) and anti-FOXO3A; anti- β -Catenin, anti-Oct4, anti-Sox2, anti-Nanog and anti-PARP-1 (Cell Signaling, Danvers, MA, USA); anti-Ars2 (Santa Cruz Biotechnology, CA, USA); anti-HO-1 (Enzo Life Sciences, Plymouth Meeting, PA, USA). The secondary antibodies were conjugated to horseradish peroxidase; signals were detected using the ECL system (Thermo Scientific, Rockford, IL, USA).

ELISA

Antibody pair used in sandwich ELISA for this study is commercially available. Kit to detect IL6 was from Life Technologies/Invitrogen (Carlsbad, CA, USA).

Statistical analysis

Data from 3 to 4 independent experiments were calculated as means and standard deviations. Comparisons of results between treated and control groups were made by the Students' *t*-tests. A *p* value of 0.05 or less between groups was considered significant.

Acknowledgments We would like to thank Drs. Adayabalam Balajee, Mercy Davidson, Peter Grabham, Bo Zhang and Howard Lieberman for advice, critical reading of manuscript and discussion. We

would like to thank Dr. E.Y. Snyder (Sanford-Burnham Research Institute, San Diego, CA) for mouse neural stem cells (clone C17.2). This work was supported by Environmental Center Grant P30 ES009089 and NIH Grant P01 CA049062.

Conflict of interest None.

References

- Vahidnia A, van der Voet GB, de Wolff FA (2007) Arsenic neurotoxicity—a review. *Hum Exp Toxicol* 26:823–832
- Chen CJ, Chen CW, Wu MM, Kuo TL (1992) Cancer potential in liver, lung, bladder and kidney due to ingested inorganic arsenic in drinking water. *Br J Cancer* 66:888–892
- Lindgren A, Danielsson BR, Dencker L, Vahter M (1984) Embryotoxicity of arsenite and arsenate: distribution in pregnant mice and monkeys and effects on embryonic cells in vitro. *Acta Pharmacol Toxicol (Cph)* 54:311–320
- Snow ET (1992) Metal carcinogenesis: mechanistic implications. *Pharmacol Ther* 53:31–65
- Pulido MD, Parrish AR (2003) Metal-induced apoptosis: mechanisms. *Mutat Res* 533:227–241
- Partridge MA, Huang SX, Hernandez-Rosa E, Davidson MM, Hei TK (2007) Arsenic induced mitochondrial DNA damage and altered mitochondrial oxidative function: implications for genotoxic mechanisms in mammalian cells. *Cancer Res* 67:5239–5247
- Hei TK, Liu SX, Waldren C (1998) Mutagenicity of arsenic in mammalian cells: role of reactive oxygen species. *Proc Natl Acad Sci USA* 95:8103–8107
- Liu SX, Athar M, Lippai I, Waldren C, Hei TK (2001) Induction of oxyradicals by arsenic: implication for mechanism of genotoxicity. *Proc Natl Acad Sci USA* 98:1643–1648
- Pardal R, Clarke MF, Morrison SJ (2003) Applying the principles of stem-cell biology to cancer. *Nat Rev Cancer* 3:895–902
- Hanna JH, Saha K, Jaenisch R (2010) Pluripotency and cellular reprogramming: facts, hypotheses, unresolved issues. *Cell* 143: 508–525
- Graf T (2011) Historical origins of transdifferentiation and reprogramming. *Cell Stem Cell* 9:504–516
- Niwa H, Ogawa K, Shimosato D, Adachi K (2009) A parallel circuit of LIF signalling pathways maintains pluripotency of mouse ES cells. *Nature* 460:118–122
- Hirai H, Karian P, Kikyo N (2011) Regulation of embryonic stem cell self-renewal and pluripotency by leukaemia inhibitory factor. *Biochem J* 438:11–23
- Ying QL, Nichols J, Chambers I, Smith A (2003) BMP induction of Id proteins suppresses differentiation and sustains embryonic stem cell self-renewal in collaboration with STAT3. *Cell* 115:281–292
- Krasilnikov M, Ivanov VN, Dong J, Ronai Z (2003) ERK and PI3K negatively regulate STAT-transcriptional activities in human melanoma cells: implications towards sensitization to apoptosis. *Oncogene* 22:4092–4101
- Menges CW, McCance DJ (2008) Constitutive activation of the Raf–MAPK pathway causes negative feedback inhibition of Ras–PI3K–AKT and cellular arrest through the EphA2 receptor. *Oncogene* 27:2934–2940
- Chen X, Xu H, Yuan P, Fang F, Huss M, Vega VB, Wong E, Orlov YL, Zhang W, Jiang J, Loh YH, Yeo HC, Yeo ZX, Narang V, Govindarajan KR, Leong B, Shahab A, Ruan Y, Bourque G, Sung WK, Clarke ND, Wei CL, Ng HH (2008) Integration of external signaling pathways with the core transcriptional network in embryonic stem cells. *Cell* 133:1106–1117

18. Takahashi K, Yamanaka S (2006) Induction of pluripotent stem cells from mouse embryonic and adult fibroblast cultures by defined factors. *Cell* 126:663–676
19. Takahashi K, Okita K, Nakagawa M, Yamanaka S (2007) Induction of pluripotent stem cells from fibroblast cultures. *Nat Protoc* 2:3081–3089
20. Yu J, Vodyanik MA, Smuga-Otto K, Antosiewicz-Bourget J, Frane JL, Tian S, Nie J, Jonsdottir GA, Ruotti V, Stewart R, Slukvin II, Thomson JA (2007) Induced pluripotent stem cell lines derived from human somatic cells. *Science* 318:1917–1920
21. Han J, Yuan P, Yang H, Zhang J, Soh BS, Li P, Lim SL, Cao S, Tay J, Orlov YL, Lufkin T, Ng HH, Tam WL, Lim B (2010) Tbx3 improves the germ-line competency of induced pluripotent stem cells. *Nature* 463:1096–1100
22. Chambers I, Tomlinson SR (2009) The transcriptional foundation of pluripotency. *Development* 136:2311–2322
23. Waalkes MP, Liu J, Diwan BA (2007) Transplacental arsenic carcinogenesis in mice. *Toxicol Appl Pharmacol* 222:271–280
24. Ivanov VN, Hei TK (2011) Regulation of apoptosis in human melanoma and neuroblastoma cells by statins, sodium arsenite and TRAIL: a role of combined treatment versus monotherapy. *Apoptosis* 16:1268–1284
25. Shen ZX, Chen GQ, Ni JH, Li XS, Xiong SM, Qiu QY, Zhu J, Tang W, Sun GL, Yang KQ, Chen Y, Zhou L, Fang ZW, Wang YT, Ma J, Zhang P, Zhang TD, Chen SJ, Chen Z, Wang ZY (1997) Use of arsenic trioxide (As₂O₃) in the treatment of acute promyelocytic leukemia (APL): II. Clinical efficacy and pharmacokinetics in relapsed patients. *Blood* 89:3354–3360
26. Ivanov VN, Hei TK (2004) Arsenite sensitizes human melanomas to apoptosis via tumor necrosis factor alpha-mediated pathway. *J Biol Chem* 279:22747–22758
27. Costantini P, Jacotot E, Decaudin D, Kroemer G (2000) Mitochondrion as a novel target of anticancer chemotherapy. *J Natl Cancer Inst* 92:1042–1053
28. Larochette N, Decaudin D, Jacotot E, Brenner C, Marzo I, Susin SA, Zamzami N, Xie Z, Reed J, Kroemer G (1999) Arsenite induces apoptosis via a direct effect on the mitochondrial permeability transition pore. *Exp Cell Res* 249:413–421
29. Fulda S, Debatin KM (2006) Extrinsic versus intrinsic apoptosis pathways in anticancer chemotherapy. *Oncogene* 25:4798–4811
30. Luo J, Manning BD, Cantley LC (2003) Targeting the PI3K–AKT pathway in human cancer: rationale and promise. *Cancer Cell* 4:257–262
31. Loberg RD, Vesely E, Brosius FC 3rd (2002) Enhanced glycogen synthase kinase-3beta activity mediates hypoxia-induced apoptosis of vascular smooth muscle cells and is prevented by glucose transport and metabolism. *J Biol Chem* 277:41667–41673
32. Cheng HY, Li P, David M, Smithgall TE, Feng L, Lieberman MW (2004) Arsenic inhibition of the JAK–STAT pathway. *Oncogene* 23:3603–3612
33. Gutierrez H, Davies AM (2011) Regulation of neural process growth, elaboration and structural plasticity by NF-kappaB. *Trends Neurosci* 34:316–325
34. Storm MP, Bone HK, Beck CG, Bourillot PY, Schreiber V, Damiano T, Nelson A, Savatier P, Welham MJ (2007) Regulation of Nanog expression by phosphoinositide 3-kinase-dependent signaling in murine embryonic stem cells. *J Biol Chem* 282:6265–6273
35. Laplante M, Sabatini DM (2012) mTOR signaling in growth control and disease. *Cell* 149:274–293
36. Snyder EY, Deitcher DL, Walsh C, Arnold-Aldea S, Hartwig EA, Cepko CL (1992) Multipotent neural cell lines can engraft and participate in development of mouse cerebellum. *Cell* 68:33–51
37. Mi R, Luo Y, Cai J, Limke TL, Rao MS, Hoke A (2005) Immortalized neural stem cells differ from nonimmortalized cortical neurospheres and cerebellar granule cell progenitors. *Exp Neurol* 194:301–319
38. Rocha RA, Gimeno-Alcaniz JV, Martin-Ibanez R, Canals JM, Velez D, Devesa V (2011) Arsenic and fluoride induce neural progenitor cell apoptosis. *Toxicol Lett* 203:237–244
39. Boeuf H, Hauss C, Graeve FD, Baran N, Keding C (1997) Leukemia inhibitory factor-dependent transcriptional activation in embryonic stem cells. *J Cell Biol* 138:1207–1217
40. Paling NR, Wheadon H, Bone HK, Welham MJ (2004) Regulation of embryonic stem cell self-renewal by phosphoinositide 3-kinase-dependent signaling. *J Biol Chem* 279:48063–48070
41. Watanabe S, Umehara H, Murayama K, Okabe M, Kimura T, Nakano T (2006) Activation of AKT signaling is sufficient to maintain pluripotency in mouse and primate embryonic stem cells. *Oncogene* 25:2697–2707
42. Groszer M, Erickson R, Scripture-Adams DD, Lesche R, Trumpp A, Zack JA, Kornblum HI, Liu X, Wu H (2001) Negative regulation of neural stem/progenitor cell proliferation by the Pten tumor suppressor gene in vivo. *Science* 294:2186–2189
43. Sato N, Meijer L, Skaltsounis L, Greengard P, Brivanlou AH (2004) Maintenance of pluripotency in human and mouse embryonic stem cells through activation of Wnt signaling by a pharmacological GSK-3-specific inhibitor. *Nat Med* 10:55–63
44. Kielman MF, Rindapaa M, Gaspar C, van Poppel N, Breukel C, van Leeuwen S, Taketo MM, Roberts S, Smits R, Fodde R (2002) Apc modulates embryonic stem-cell differentiation by controlling the dosage of beta-catenin signaling. *Nat Genet* 32:594–605
45. Le Belle JE, Orozco NM, Paucar AA, Saxe JP, Mottahedeh J, Pyle AD, Wu H, Kornblum HI (2011) Proliferative neural stem cells have high endogenous ROS levels that regulate self-renewal and neurogenesis in a PI3K/AKT-dependant manner. *Cell Stem Cell* 8:59–71
46. Vivanco I, Sawyers CL (2002) The phosphatidylinositol 3-kinase AKT pathway in human cancer. *Nat Rev Cancer* 2:489–501
47. Ivanov VN, Hei TK (2006) Sodium arsenite accelerates TRAIL-mediated apoptosis in melanoma cells through upregulation of TRAIL-R1/R2 surface levels and downregulation of cFLIP expression. *Exp Cell Res* 312:4120–4138
48. Bode AM, Dong Z (2002) The paradox of arsenic: molecular mechanisms of cell transformation and chemotherapeutic effects. *Crit Rev Oncol Hematol* 42:5–24
49. Kapahi P, Takahashi T, Natoli G, Adams SR, Chen Y, Tsien RY, Karin M (2000) Inhibition of NF-kappa B activation by arsenite through reaction with a critical cysteine in the activation loop of Ikkappa B kinase. *J Biol Chem* 275:36062–36066
50. Covacu R, Arvidsson L, Andersson A, Khademi M, Erlandsson-Harris H, Harris RA, Svensson MA, Olsson T, Brundin L (2009) TLR activation induces TNF-alpha production from adult neural stem/progenitor cells. *J Immunol* 182:6889–6895
51. Yang J, Liao X, Agarwal MK, Barnes L, Auron PE, Stark GR (2007) Unphosphorylated STAT3 accumulates in response to IL-6 and activates transcription by binding to NFkappaB. *Genes Dev* 21:1396–1408
52. Torres J, Watt FM (2008) Nanog maintains pluripotency of mouse embryonic stem cells by inhibiting NFkappaB and cooperating with Stat3. *Nat Cell Biol* 10:194–201
53. Pession A, Tonelli R (2005) The MYCN oncogene as a specific and selective drug target for peripheral and central nervous system tumors. *Curr Cancer Drug Targets* 5:273–283
54. Pettersson H, Karlsson J, Pietras A, Øra I, Pålman S (2007) Arsenic trioxide and neuroblastoma cytotoxicity. *J Bioenerg Biomembr* 39:35–41